# Extension of the Time-Spectral Approach to Overset Solvers for Arbitrary Motion

Joshua I. Leffell*
*Stanford University, Stanford, CA 94035*

Scott M. Murman†
*NASA Ames Research Center, Moffett Field, CA 94035*

Thomas H. Pulliam‡
*NASA Ames Research Center, Moffett Field, CA 94035*

## I. Introduction

Forced periodic flows arise in a broad range of aerodynamic applications such as rotorcraft, turbomachinery, and flapping wing configurations. Standard practice involves solving the unsteady flow equations forward in time until the initial transient exits the domain and a statistically stationary flow is achieved. It is often required to simulate through several periods to remove the initial transient making unsteady design optimization prohibitively expensive for most realistic problems. An effort to reduce the computational cost of these calculations led to the development of the Harmonic Balance method [1, 2] which capitalizes on the periodic nature of the solution. The approach exploits the fact that forced temporally periodic flow, while varying in the time domain, is invariant in the frequency domain. Expanding the temporal variation at each spatial node into a Fourier series transforms the unsteady governing equations into a steady set of equations in integer harmonics that can be tackled with the acceleration techniques afforded to steady-state flow solvers. Other similar approaches, such as the Nonlinear Frequency Domain [3,4,5], Reduced Frequency [6] and Time-Spectral [7, 8, 9] methods, were developed shortly thereafter. Additionally, adjoint-based optimization techniques can be applied [10, 11] as well as frequency-adaptive methods [12, 13, 14] to provide even more flexibility to the method. The Fourier temporal basis functions imply spectral convergence as the number of harmonic modes, and correspondingly number of time samples, $N$, is increased. Some elect to solve the equations in the frequency domain directly, while others choose to transform the equations back into the time domain to simplify the process of adding this capability to existing solvers, but each harnesses the underlying steady solution in the frequency domain. These temporal projection methods will herein be collectively referred to as *Time-Spectral* methods.

Time-Spectral methods have demonstrated marked success in reducing the computational costs associated with simulating periodic forced flows, but have yet to be fully applied to overset or Cartesian solvers for arbitrary motion with dynamic hole-cutting. Overset and Cartesian grid methodologies are versatile techniques capable of handling complex geometry configurations in practical engineering applications, and the combination of the Time-Spectral approach with this general capability potentially provides an enabling new design and analysis tool. In an arbitrary moving-body scenario for these approaches, a Lagrangian body moves through a fixed Eulerian mesh and mesh points in the Eulerian mesh interior to the solid body are removed (*cut* or *blanked*), leaving a *hole* in the Eulerian mesh. During the dynamic motion some gridpoints in the domain are blanked and do not have a complete set of time-samples preventing a direct implementation of the Time-Spectral method. Murman[6] demonstrated the Time-Spectral approach for a Cartesian solver with a rigid domain motion, wherein the hole cutting remains constant. Similarly, Custer et al. [15, 16] used the NASA overset OVERFLOW solver and limited the amount of relative motion to ensure static hole-cutting and interpolation. Recently, Mavriplis and Mundis[17] demonstrated a qualitative method for applying the Time-Spectral approach to an unstructured overset solver for arbitrary motion.

*Graduate Student, Department of Aeronautics & Astronautics, AIAA Student Member. jleffell@stanford.edu
†Senior Research Scientist, AIAA Member. Scott.M.Murman@nasa.gov
‡Senior Research Scientist, AIAA Associate Fellow. Thomas.H.Pulliam@nasa.gov

The goal of the current work is to develop a robust and general method for handling arbitrary motion with the Time-Spectral approach within an overset or Cartesian mesh method, while still approaching the spectral convergence rate of the original Time-Spectral approach. The viscous OVERFLOW solver will be augmented with the new Time-Spectral algorithm and the capability of the method for benchmark problems in rotorcraft and turbomachinery will be demonstrated.

This abstract begins with a brief synopsis of the Time-Spectral approach for overset grids and provides details of the current approach to allow for arbitrary motion. Model problem results in one and two dimensions are included to demonstrate the viability of the method and the convergence properties. Section IV briefly outlines the implementation into the OVERFLOW solver, and the abstract closes with a description of the benchmark test cases which will be included in the final paper.

## II. Extension of Time-Spectral Method for Overset Solution Procedures

The fundamental issue of providing Time-Spectral capabilities to an overset solver concerns the nodes that dynamically move in and out of the physical domain as a function of the relative motion between the surface geometry and the background Eulerian grid(s). Projection into the frequency domain has infinite support in time requiring special treatment for these nodes. Figure 1 demonstrates the issue for a figurative case of a one-dimensional piston moving in a sinusoidal path.

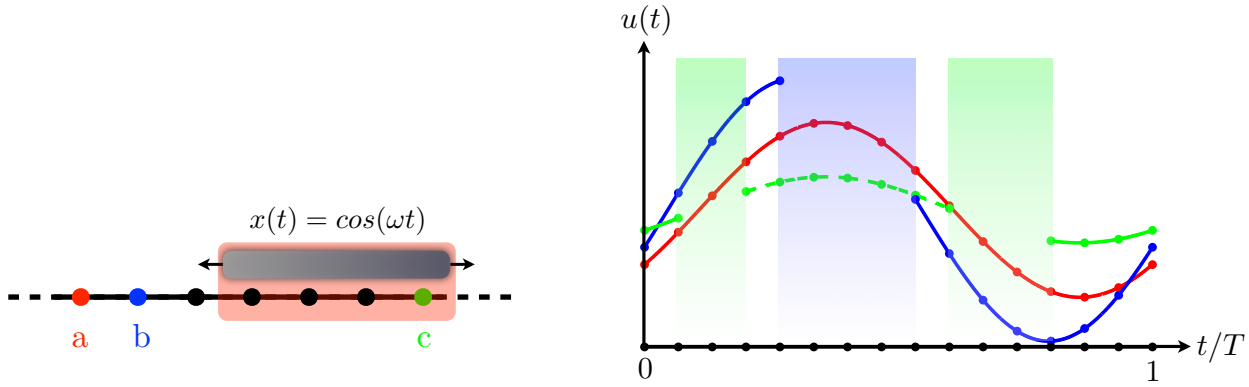


(a) Piston Motion (b) Solution Time Histories

Figure 1: Figurative piston trajectory and solution histories. The piston "cuts" nodes as it oscillates over the fictional grid in Fig. 1a. Shaded regions in 1b represent blanked intervals through which the solution is undefined for nodes of the corresponding color.

Fictional solutions at nodes $a$, $b$ and $c$ in Fig. 1a demonstrate dynamic hole cutting by the relative motion of the piston. The piston never reaches node $a$ and thus its solution is continuous for the entire time-history of the period. The piston blanks node $b$ briefly during the middle of the period and node $c$ twice. Thus, node $b$ has one non-periodic time interval associated with it while node $c$ has two - one each represented by the solid and hashed lines. The shaded regions serve to highlight the time over which each node lies outside the physical domain with an undefined solution. Thus, special treatment is required for nodes $b$ and $c$ while the standard Time-Spectral approach can be applied to node $a$.

For a brief review of the standard Time-Spectral approach consider a general time-dependent scalar ODE:

$$\frac{\partial u}{\partial t} + R(u) = 0 \tag{1}$$

The continuous solution is projected ($\hat{\mathbf{u}} = \Phi^{-1}\mathbf{u}$) into the frequency domain,

$$\Phi_{jk} = \phi_k(t_j) = e^{i\omega k t_j} \tag{2}$$

from data at equispaced time samples, $\Delta t = \frac{2\pi}{\omega N}$, $t_j = j\Delta t$. The derivative operator is applied in the frequency domain, i.e. $\frac{d}{dt}\hat{u}_k = i\omega k \hat{u}_k$, and the result is projected back into the time domain leading to

$$\Phi D \Phi^{-1}\mathbf{u} + \mathbf{R}(\mathbf{u}) = 0 \tag{3}$$

where $\mathcal{D} = \Phi D \Phi^{-1}$ is the transformed differentiation operator[a]. Direct assembly of the transformed differential operator, $\mathcal{D}$, is derived in [7, 8]. Iterating Eq. 3 in pseudotime, $\tau$, provides a steady-state solution procedure to an underlying unsteady, yet periodic, problem,

$$\frac{d}{d\tau}\mathbf{u} + \mathcal{D}\mathbf{u} + \mathbf{R}(\mathbf{u}) = 0 \tag{4}$$

The majority of spatial nodes in an overset or Cartesian simulation will be treated with this standard procedure, but a highly accurate and robust treatment is still needed for the complement of nodes that undergo dynamic blanking. A natural approach is to fill the blanked nodes with solution data via spatial averaging and proceed with the standard Time-Spectral method (cf. [17]). While attractive for its simplicity, this approach is inconsistent as it propagates non-physical information provided by an alternative governing equation (spatial smoothing governed by Laplace's equation) into the physical domain via the infinite support of the spectral basis. This is demonstrated by solving the linear advection equation

$$\frac{\partial u}{\partial t} + a\frac{\partial u}{\partial x} = 0 \tag{5}$$

given $u(x, 0) = \sin(\omega x)$ and $u(0, t) = -\sin(\omega a t)$ for $x \in [a, b]$. The analytic solution is $u(x, t) = sin(\omega(x - at))$. The "geometry" is modeled by a gap in $x$ through which the solution and analytic residual are linearly interpolated at every step. The interpolation error across the spatial gap (Fig. 2a) at one time-sample corrupts the solution throughout the period (Fig. 2b) via the infinite support of the spectral basis. Additionally, spatial interpolation inhibits the expected temporal convergence as demonstrated in Fig. 2c.

Instead of spatial averaging, the current method partitions the time history into intervals of contiguously unblanked time samples and thus abandons the global temporal support for nodes exhibiting dynamic blanking (See Fig. 1b). This is consistent with the physics of disjoint domains separated by an impermeable boundary. It is important to note that these temporal partitions must still be evaluated on a uniform lattice to avoid manipulating the spatial operator. Thus, we seek a robust and efficient method for evaluating the temporal derivatives for non-periodic functions on a uniform lattice.

Several approaches are evaluated to achieve this goal. One option would be to compute derivatives with finite-differences or a localized differentiable basis such as wavelets. However, compact bases offer limited accuracy [18] and wavelet differentiation requires special treatment at non-periodic interval boundaries [19]. Temporal extrapolation techniques are another option that fill artificial data in the undefined portion of the given period using data from the physical portion of the time signal. Fourier continuation which extrapolates a non-periodic function into a periodic function on a larger domain [20, 21, 22], and compressed sampling that employs $L_1$ minimization to solve an underdetermined system [23], are both too costly and lack the requisite robustness. The current approach projects the solution of the unblanked nodes within a single partition onto a global basis spanning the same interval. The constraint of evenly-spaced temporal collocation points eliminates traditional optimally-accurate orthogonal polynomials (*e.g.* Chebyshev) due to Runge's phenomenon at the endpoints. Least-squares projections of orthogonal polynomials are more stable but expensive, and result in an overdetermined system whose projection does not interpolate the solution data. Rational polynomials are offered as a viable alternative for highly accurate approximations on evenly-spaced grids [24] and will be employed in the current work as they posses the properties of discrete orthogonality and spectral-like approximation order. An alternate basis may prove more successful in the future so the current approach will be kept general enough to use any projection operator, provided the corresponding analytic differentiation operator is available. In this work, solutions across each non-periodic interval are projected onto a basis of rational polynomials and differentiated accordingly. Fully periodic intervals are still projected in the Fourier basis, resulting in a hybrid approach that employs the optimal available basis.

Floater and Hormann [25] introduced a set of barycentric rational polynomials with high rates of convergence and no poles. Additional efforts to explore rational polynomials and their utility as a pseudospectral basis for spectral collocation methods include but are not limited to [26, 27, 28, 29]. Tee and Trefethen [30]

[a]Alternatively, the residual operator can also be projected into the frequency domain, and the resulting equations solved iteratively in the frequency domain [3, 6]. This approach takes advantage of the Fast Fourier Transform which is an $N \log N$ operation as opposed to the $N^2$ matrix operation in Eq. 3. However, for the small $N$ ($O(10 - 100)$) typically encountered in practical 3D Time-Spectral applications the difference is minimal and the time domain formulation proves more flexible

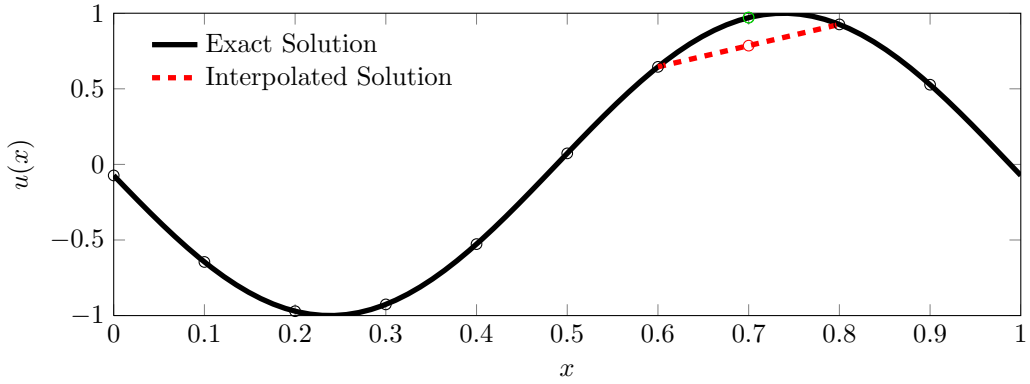


(a) "Geometry" gap and interpolation region

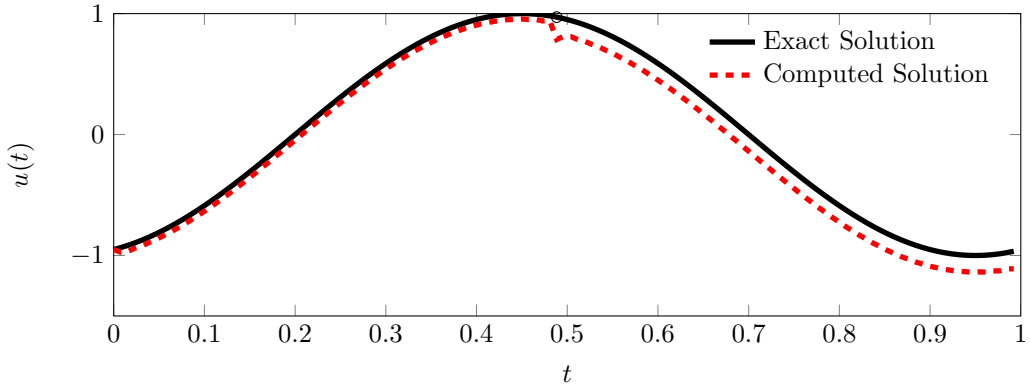


(b) Exact and computed solutions

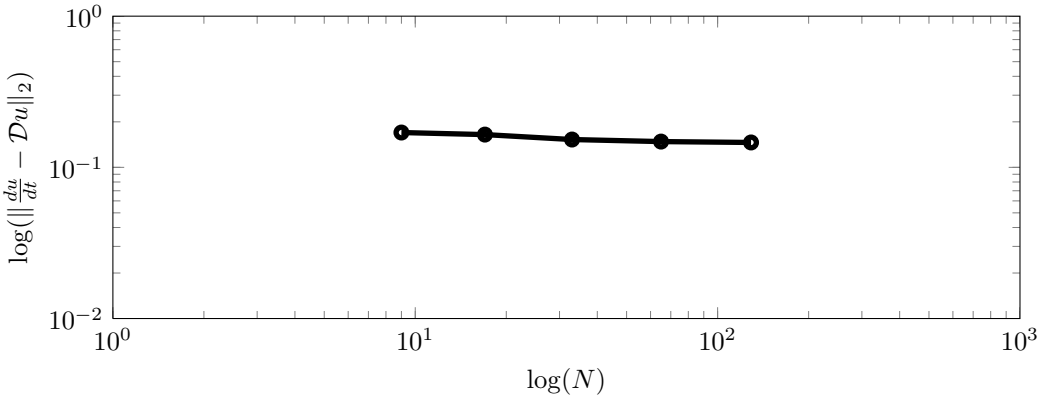


(c) Convergence with $N$

Figure 2: Spatial smoothing Time-Spectral approach

offer the following definitions for the rational interpolant, $r(x)$, in barycentric form:

$$r(x) = \frac{\sum_{k=0}^{N} \frac{w_k}{x-x_k} f_k}{\sum_{k=0}^{N} \frac{w_k}{x-x_k}} \tag{6}$$

and its corresponding differentiation operator, $D$, such that $\frac{d}{dx}\mathbf{r} = D\mathbf{r}$ where $r_k = r(x_k)$:

$$D_{jk} = \begin{cases} \frac{w_k}{w_j(x_j - x_k)} & \text{if } j \neq k \\ -\sum_{i=0, i\neq k}^{N} D_{ji} & \text{if } j = k \end{cases}$$

The interpolation is reformulated as a weighted sum of nodal basis functions with the weights equal to the function value at the nodes $\hat{f}_k = f(x_k)$:

$$f(x) = \sum_{k=0}^{N} \hat{f}_k \phi_k(x), \quad \text{with } \phi_k(x) = \frac{\frac{w_k}{x-x_k}}{\sum_{k=0}^{N} \frac{w_k}{x-x_k}} \tag{7}$$

Since barycentric rational polynomials interpolate the solution data, the transformation operator is the identity matrix, $\Phi_{jk} = \phi_k(x_j) = \delta_{jk}$, implying discrete orthogonality. It follows that the transformed differentiation operator is identical to $D$: $\mathcal{D} = \Phi D \Phi^{-1} = D$. The weights, $w_k$, control the approximation and stability characteristics of the rational interpolant and are provided by Floater and Hormann [25] to avoid poles and provide an approximation order of $d$.

Given $N+1$ samples choose the desired approximation order $d$ and define:

$$I_T := \{0, 1, ..., N-d\} \text{ and } J_\alpha := \{i \in I_T : \alpha - d \leq i \leq \alpha\} \tag{8}$$

Weights guaranteeing an absence of poles are defined by:

$$w_k = (-1)^{k-d} \sum_{i \in J_k} \prod_{j=i, j\neq k}^{i+d} \frac{1}{|x_k - x_j|} \tag{9}$$

Readers are directed to the derivation in [25] for additional details. An example of three basis functions corresponding to the first, second and fourth nodes with approximation order, $d = 3$, over 8 sample points ($N = 7$) is provided in Fig. 3 with the values at the nodes highlighted with circles. Note the interpolation property of the basis, $\phi_k(x_j) = \delta_{jk}$.

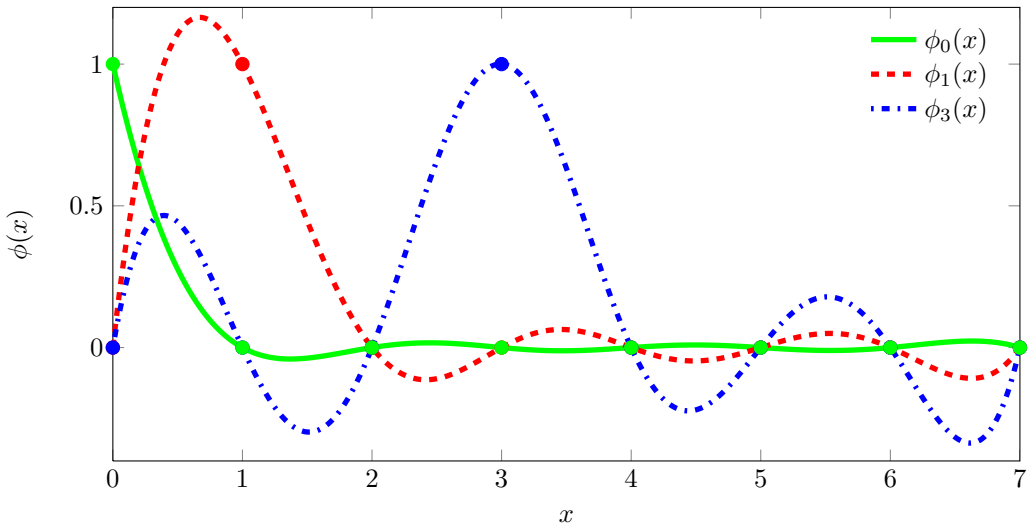


Figure 3: Rational polynomial basis functions $\phi_0(x)$, $\phi_1(x)$ and $\phi_3(x)$ corresponding to nodes 0, 1 and 3, respectively, for approximation order, $d = 3$, and 8 sampling points.

Approximation and differentiation performance of the rationals are compared to third-order finite differences, the Fourier basis, least-squares approximation using orthogonal polynomials on evenly-spaced nodes ($M \leq 2\sqrt{N}$) and Chebyshev polynomials on Chebyshev nodes in Fig. 4. An even-odd harmonic function and Runge's function (designed to expose numerical instabilities) are differentiated by each of the aforementioned methods, along with convergence of differentiation error, $e = \|\frac{df}{dx} - \mathcal{D}f\|_2$, with increasing $N$. Fourier differentiation is not applied to the aperiodic Runge's function. The approximation order for the rationals is selected as $d = \min(\lfloor \frac{1}{3}N \rfloor + 1, 10)$ for this case, but optimal selection is problem dependent and an area of continuing research [29]. The rational polynomials approach spectral convergence for both the periodic and non-periodic problems.

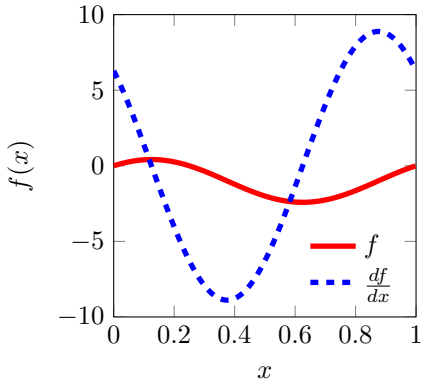


(a) Analytic function and derivative for $f(x) = \cos(\omega t) + \sin(\omega t)$

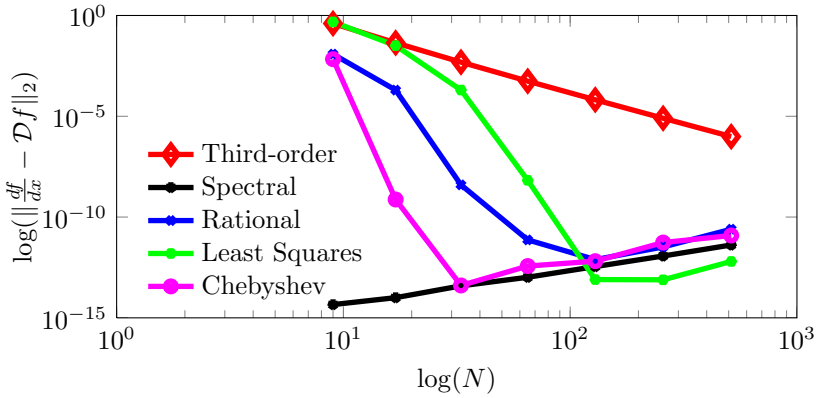


(b) Convergence of differentiation operators on periodic function

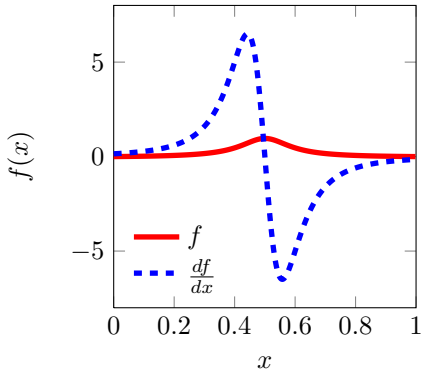


(c) Analytic function and derivative for $f(x) = \frac{1}{1+25x^2}$

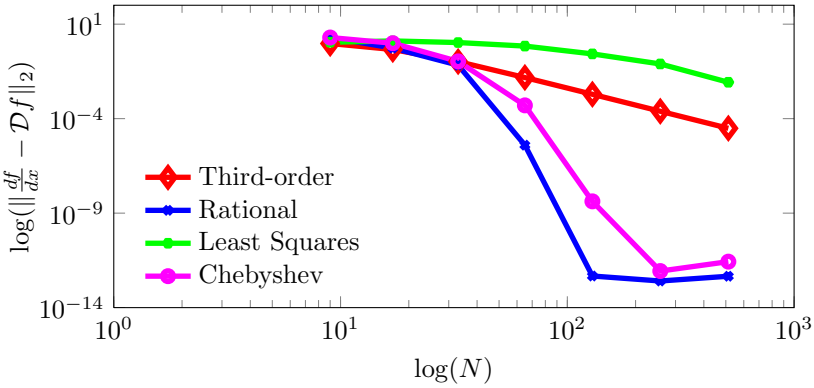


(d) Convergence of differentiation operators on Runge's function

Figure 4: Convergence of differentiated periodic and non-periodic functions

## III. Linear Advection Test Case using the Hybrid Time-Spectral Approach

A linear advection equation is used to test the hybrid Time-Spectral strategy. The barycentric rational polynomial temporal differentiation operator, $\mathcal{D}_r$, will be used on the spatial nodes blanked over some duration of the period and the Fourier differentiation operator, $\mathcal{D}_f$, is used on nodes with a periodic interval. Information propagates from left to right with wave speed, $a = 1$, and thus analytic boundary conditions are supplied at $x = 0$ and along the right edge of the blanked region. The domain is discretized with $N_x = 101$ points in space and $N = 21$ time samples. Flow is initialized uniformly to zero outside the boundary nodes and third-order finite differences are used to approximate spatial derivatives with results plotted in Fig. 5.

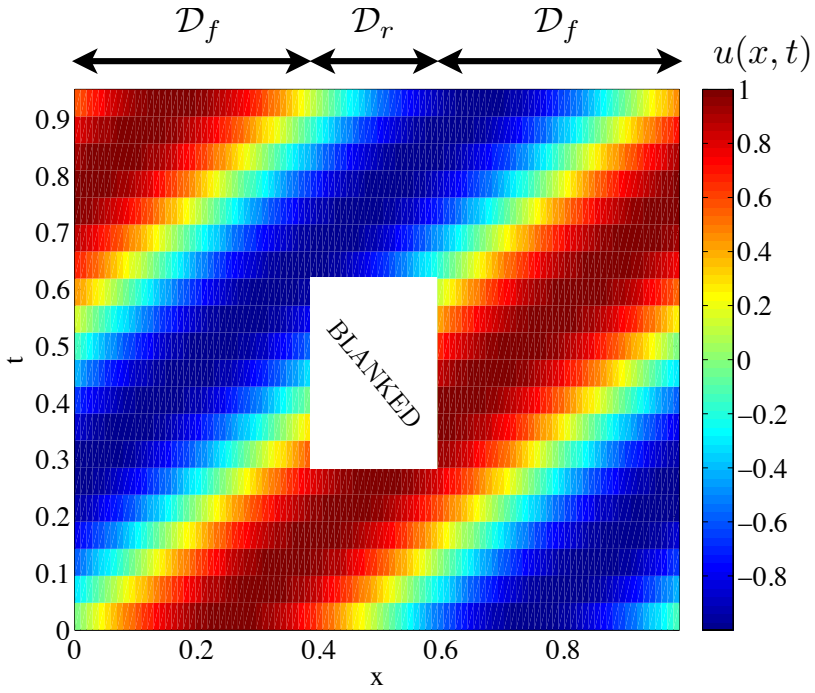


(a) Complete space-time solution

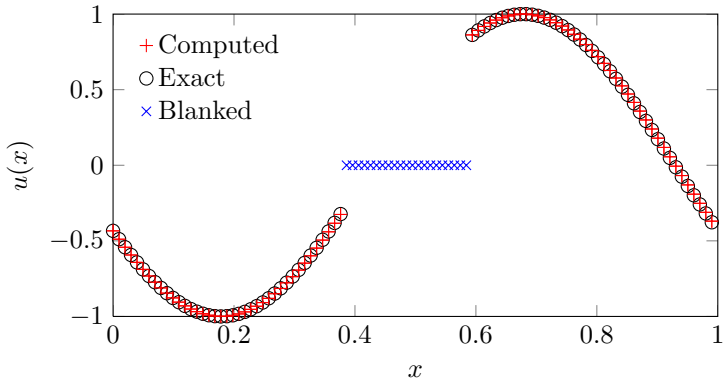


(b) Solution and blanked interval at fixed time $t = 0.4286$

Figure 5: Solution for linear advection test problem using the hybrid Fourier-rational polynomial Time-Spectral approach. The rational polynomial differentiation operator, $\mathcal{D}_r$, is applied to nodes in the central region of the domain that undergo blanking and the Fourier differentiation operator, $\mathcal{D}_f$, is applied elsewhere.

The maximum error in the blanked simulation is actually lower than the unblanked case ($7.717 \times 10^{-3}$ vs $7.757 \times 10^{-3}$) due to the analytic solution boundary condition on the right side of the blanked region. The largest solution difference upwind of the analytic boundary was $7.861 \times 10^{-4}$ demonstrating that the Fourier-rational hybrid approach essentially produces the same result in the unblanked region for this simple test problem. The same approach will be used in the hybrid Time-Spectral OVERFLOW overset solver, as discussed in the following section.

## IV. Implementation of Time-Spectral Approach in OVERFLOW

One of the strengths of the Time-Spectral approach is that the spatial operator remains unchanged, making the scheme straightforward to add and maintain in existing code. The current work leverages the OVERFLOW overset flow solver [31], which provides a mature code base for solving the three-dimensional compressible Reynolds-averaged Navier-Stokes (RANS) equations using a structured finite-difference scheme. OVERFLOW uses an approximate-factorization algorithm for the implicit solution of the spatial derivatives,

and the Time-Spectral operator is easily integrated with this approach by the addition of a similar factored operator for the time derivative. This avoids forming and solving a $N_x^3 \times N_Q \times N$ system of equations coupled across time and space. Writing the full Time-Spectral approximate-factorization difference equation in "delta" form gives,

$$[I + \Delta\tau A_x]\,[I + \Delta\tau A_y]\,[I + \Delta\tau A_z]\,[I + \Delta\tau A_t]\,\Delta\vec{Q} \quad = \quad -\Delta\tau\left(R(\vec{Q}^n) + S(\vec{Q}^n)\right) \tag{10}$$

where $R(\vec{Q}^n)$ is the standard spatial residual operator, and $S(\vec{Q}^n)$ is the Time-Spectral differential operator applied to the state vector at time level $n$. $A_x$, $A_y$ and $A_z$ are the linearized spatial operators corresponding to the $x-$, $y-$ and $z-$directions and $A_t = \mathcal{D}$ is the temporal differentiation operator. The Time-Spectral approach as applied to OVERFLOW retains the identical spatial residual operator and avoids modifying the existing implicit operator because they are applied one time-sample at a time. The required modifications are limited to an additional linear solve (of dimension $N$) for the Time-Spectral factored operator and computation of the source term. In other words, time is treated as an additional spatial dimension when solving for the steady state in the combined space-time domain.

The computational memory requirements for a Time-Spectral solution are greater than a standard unsteady case because the solution and source term must be stored for each time sample. However, careful implementation limits the storage requirements and allows for a significant number of temporal modes even in complex three-dimensional problems. Ignoring the trivial storage and processing associated with the hole cutting, the current implementation in OVERFLOW stores a copy of the state vector $Q^n$ and Time-Spectral source term $S(Q^n)$ at each time level, along with an additional working copy of the grid and metrics. Thus, the total *additional* storage is $2N_x^3 N_Q N + 12N_x^3$, where $N_x$ and $N$ represent the number of spatial and temporal modes, respectively, and $N_Q$ is the number of conserved solution variables. An additional cost of the approximate-factored matrix for the temporal derivative is also accounted for depending upon the relative size of $N_x$ and $N$. Using a target problem size of $N_x^3 = 125$M grid points, which is representative of a three-dimensional rotorcraft or turbomachinery simulation, and 125 8-core Intel Nehalem nodes of the NASA Pleiades supercomputer, Fig. 6 shows the variation in total memory with number of temporal modes for our target problem. As seen, even limiting to 125 compute nodes there is still sufficient memory for up to 200 temporal modes, and larger problems similarly benefit from the favorable scaling.

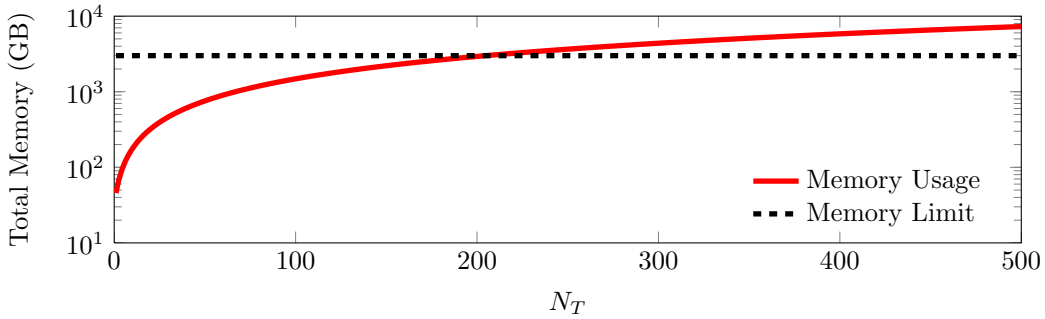


Figure 6: Total Memory Storage (GB) versus $N$ for 125 Intel Nehalem Nodes on the Pleiades supercomputer

## V. Final Paper

As mentioned in the Introduction, the Time-Spectral approach within OVERFLOW has already been demonstrated by Custer et al. [15, 16], and as such the current work to-date has focused on developing the necessary numerics of the Time-Spectral approach for disjoint domains using the rational polynomial bases. The use of the rational polynomial differential operator in an implicit two-factor scheme leads to a conditionally stable algorithm. When combined with the spatial operators in a multi-dimensional finite-difference scheme, as above, the numerical dissipation of the spatial operators can move all the unstable modes left of the imaginary axis. This is similar to the behavior when using the implicit Euler time integration in a two-factor scheme [32]. In practice the conditional stability of the rational polynomial operator does not appear more restrictive than the existing stability constraints of the spatial operator, however, a complete stability analysis of the rational polynomial scheme will be included in the full paper.

Three benchmark two-dimensional problems are targeted for inclusion in the full paper. First, unsteady and Time Spectral simulations on single and overset grids are computed for an inviscid transonic oscillating NACA 0012 airfoil and compared to experimental data found in [33] followed by a periodic tri-rotor configuration (See Fig. 7) and a stator-rotor-stator configuration (Fig. 8).

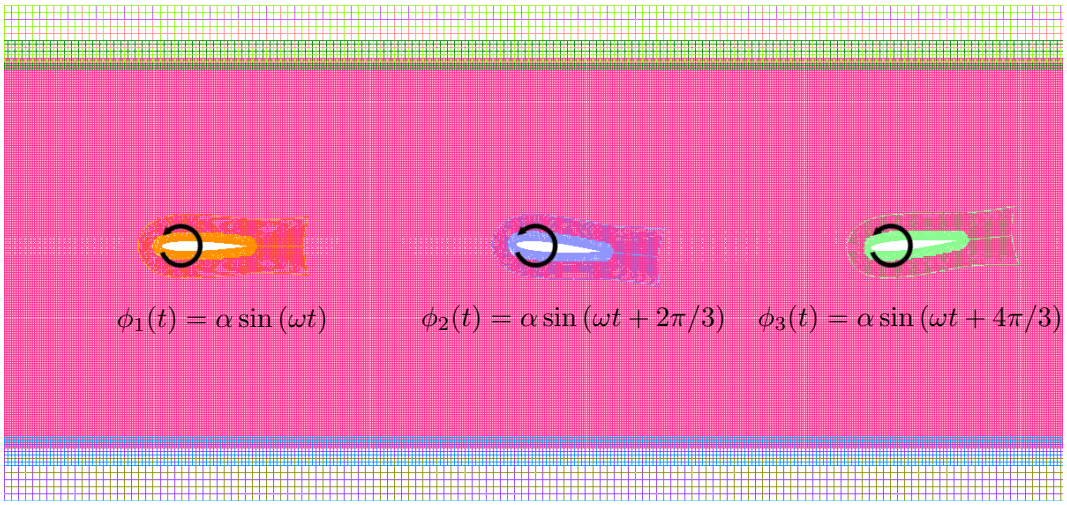


Figure 7: Two-dimensional tandem airfoil configuration. Flowfield is periodic in freestream direction to simulate a rotorcraft system in two-dimensions.

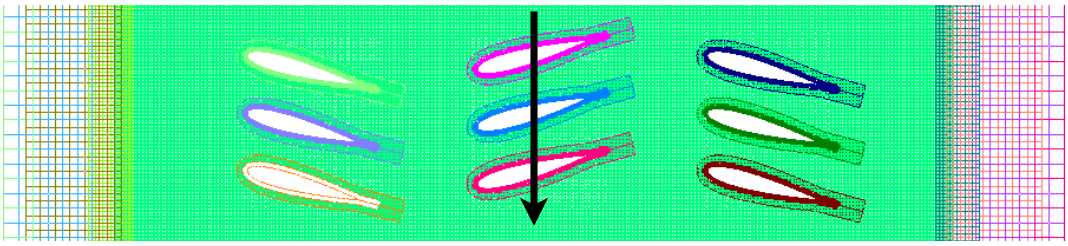

Figure 8: Example stator-rotor-stator configuration where rotor moves down relative to the stators.

These problems are representative of more complex three-dimensional applications, while still computationally tractable for a rigorous analysis. Further, the rotor-stator configuration contains benchmark experimental data [34]. In particular we are interested in the ability of the Time-Spectral approach to capture the complex wake interactions, and associated broad-spectrum frequency response, when using hybrid-RANS or LES turbulence modeling approaches for these problems. These computational studies will be included in the full paper.

## References

[1]Hall, K., Thomas, J., and Clark, W., "Computation of Unsteady Nonlinear Flows in Cascades using a Harmonic Balance Technique," 9th international symposium on unsteady aerodynamics, aeroacoustics and aeroelasticity of turbomachines, Lyon, France, September 2000.

[2]Hall, K., Thomas, J., and Clark, W., "Computation of Unsteady Nonlinear Flows in Cascades using a Harmonic Balance Technique," *AIAA Journal*, Vol. 40, 2002, pp. 879–886.

[3]McMullen, M. S. and Jameson, A., "The Computational Efficiency of Non-Linear Frequency Domain Methods," *Journal of Computational Physics*, Vol. 212, 2006, pp. 637–661.

[4]McMullen, M., Jameson, A., and Alonso, J., "Demonstration of Nonlinear Frequency Domain Methods," *AIAA Journal*, Vol. 44, No. 7, July 2006, pp. 1428–1435.

[5]Nadarajah, S. K., McMullen, M. S., and Jameson, A., "Optimum Shape Design for Unsteady Flow Using Time Accurate and Non-Linear Frequency Domain Methods," AIAA Paper 3875, June 2003.

[6]Murman, S. M., "A Reduced-Frequency Approach for Calculating Dynamic Derivatives," *AIAA Journal*, Vol. 45, No. 6, June 2007, pp. 1161–1168.

[7]Gopinath, A. K. and Jameson, A., "Time Spectral Method for Periodic Unsteady Computations over Two- and Three-Dimensional Bodies," AIAA Paper 2005-1220, January 2005.

[8]Gopinath, A. K. and Jameson, A., "Application of the Time Spectral Method to Periodic Vortex Shedding," AIAA Paper 2006-0449, January 2006.

[9]Blanc, F., Roux, F.-X., Jouhaud, J.-C., and Boussuge, J.-F., "Numerical Methods for Control Surfaces Aerodynamics with Flexibility Effects," *IFASD*, 2009.

[10]Choi, S., Potsdam, M., Lee, K., Iaccarino, G., and Alonso, J. J., "Helicopter Rotor Design Using a Time-Spectral and Adjoint-Based Method," AIAA Paper 5810, September 2008.

[11]Nadarajah, S. K. and Tatossian, C. A., "Adjoint-Based Aerodynamic Shape Optimization of Rotorcraft Blades," AIAA Paper 6730, August 2008.

[12]Mosahebi, A. and Nadarajah, S. K., "An Implicit Adaptive Non-Linear Frequency Domain Method (pNLFD) for Viscous Periodic Steady State Flows on Deformable Grids," AIAA Paper 0775, January 2011.

[13]Maple, R. C., King, P. I., Wolff, J. M., and Orkwis, P. D., "Split-Domain Harmonic Balance Solutions to Burger's Equation for Large-Amplitude Distrubances," *AIAA Journal*, Vol. 41, No. 2, February 2003, pp. 206–212.

[14]Maple, R. C., King, P. I., and Oxley, M. E., "Adaptive Harmonic Balance Solutions to Euler's Equation," *AIAA Journal*, Vol. 41, No. 9, September 2003, pp. 1705–1714.

[15]Thomas, J. P., Custer, C. H., Dowell, E. H., and Hall, K. C., "Unsteady Flow Computation Using a Harmonic Balance Approach Implemented about the OVERFLOW 2 Flow Solver," AIAA Paper 2009-4270, June 2009.

[16]Custer, C. H., *A Nonlinear Harmonic Balance Solver for an Implicit CFD Code: OVERFLOW 2*, Ph.D. thesis, Duke University, 2009.

[17]Mavriplis, D. and Mundis, N., "Extensions of Time Spectral Methods for Practical Rotorcraft Problems," AIAA Paper 2012-0423, January 2012.

[18]Strang, G., "The Optimal Coefficients in Daubechies Wavelets," *Physica D*, Vol. 60, 1992, pp. 239–244.

[19]Romine, C. and Peyton, B., "Computing Connection Coefficients of Compactly Supported Wavelets on Bounded Intervals," Mathematical Sciences Section ORNL/TM-13413, Oak Ridge National Laboratory, April 1997.

[20]Huybrechs, D., "On the Fourier Extension of Nonperiodic Functions," *SIAM Journal of Numerical Analysis*, Vol. 47, No. 6, 2010, pp. 4326–4355.

[21]Boyd, J. P., "A Comparison of Numerical Algorithms for Fourier Extension of the First, Second, and Third Kinds," *Journal of Computational Physics*, Vol. 178, 2002, pp. 118–160.

[22]Bruno, O., Han, Y., and Pohlman, M. M., "Accurate, High-Order Representation of Complex Three-Dimensional Surfaces via Fourier Continuation Analysis," *Journal of Computational Physics*, Vol. 227, 2007, pp. 1094–1125.

[23]Candes, E., "Compressive Sampling," International Congress of Mathematicians, 2006.

[24]Platte, R. B., Trefethen, L. N., and Kuijlaars, A. B., "Impossibility of Fast Stable Approximations of Analytic Functions from Equispaced Samples," *SIAM Review*, Vol. 53, No. 2, 2011, pp. 308–18.

[25]Floater, M. S. and Hormann, K., "Barycentric Rational Interpolation with No Poles and High Rates of Approximation," *Numerische Mathematik*, Vol. 107, No. 2, August 2007, pp. 315–331.

[26]Baltensperger, R. and Berrut, J.-P., "The Linear Rational Collocation Method," *Journal of Computational and Applied Math*, Vol. 134, 2001, pp. 243–258.

[27]Berrut, J.-P. and Baltensperger, R., "The Linear Rational Pseudospectral Method for Boundary Value Problems," *BIT*, Vol. 41, No. 5, 2001, pp. 868–879.

[28]Bos, L., Marchi, S. D., Hormann, K., and Klein, G., "On the Lebesgue Constant of Barycentric Rational Interpolation at Equidistant Nodes," *Journal of Computational and Applied Math*, 2011.

[29]Klein, G., "An Extension of the Floater-Hormann Family of Barycentric Rational Interpolants," *Mathematics of Computation*, to appear, 2012.

[30]Tee, T. and Trefethen, L. N., "A Rational Spectral Collocation Method with Adaptively Transformed Chebyshev Grid Points," *SIAM Journal of Scientific Computing*, Vol. 28, No. 5, 2006, pp. 1798–1811.

[31]Nichols, R. and Buning, P., "Solver and Turbulence Model Upgrades to OVERFLOW 2 for Unsteady and High Speed Applications," AIAA Paper 2824, 2006.

[32]Lomax, H., Pulliam, T. H., and Zingg, D. W., *Fundamentals of Computational Fluid Dynamics*, Springer, Berlin, 2001.

[33]Landon, R., "Compendium of Unsteady Aerodynamic Measurements," AGARD Report No. 702, August 1982.

[34]Dring, R., Joslyn, H., Hardin, L., and Wagner, J., "Turbine Rotor-Stator Interaction," *ASME Journal of Engineering for Power*, Vol. 104, 1982, pp. 729–742.